JOURNAL OF GEOPHYSICAL RESEARCH, VOL. 102, NO. B4, PAGES 8105–8120, APRIL 10, 1997

Influence of change in physical state on elastic nonlinear response in rock: Significance of effective pressure and water saturation

Bernard Zinszner
Institut Français du Pétrole, Rueil Malmaison, France

Paul A. Johnson[1]
Earth and Environmental Sciences Division, Los Alamos National Laboratory, Los Alamos, New Mexico

Patrick N. J. Rasolofosaon
Institut Français du Pétrole, Rueil Malmaison, France

Abstract. We describe Young's mode resonant bar results obtained under effective pressure at two saturation states: dry and water saturated. We monitor primary manifestations of nonlinear response in these experiments: the harmonic content, the source extinction intensity, and fundamental resonant frequency shift. In addition, we describe the hysteretic behavior of the static pressure response, the linear modulus, and Q. Because we currently lack a complete theoretical description of nonlinear behavior under resonance at pressure, we provide relative measures of nonlinear response rather than absolute values. The rocks include Fontainebleau and Meule sandstones and Lavoux limestone. Dynamic strain levels range from 10^{-8} to 10^{-5} and frequencies range from 1 to 10 kHz. The elastic nonlinear response of each of the rocks is markedly different over the range of physical property states explored. The different responses are related to differences in mechanical response resulting from rock type, grain cement type, etc. In all of the samples studied, the change in resonant frequency as a function of excitation intensity is not measurable above approximately 10 MPa; however, harmonics are observed at larger effective pressure levels. Hysteresis in velocity and Q versus pressure vary considerably between the rocks. The effect of Q on the experiments is marked. When Q is low (<10) as for some saturated samples, relative excitations must be large in order to induce equivalent dry sample strains.

Introduction

Our primary goal in this work is describing and understanding the evolution of elastic nonlinear response of rock under effective pressure under different water saturation states (dry and water saturated), with the ultimate goal of geophysical/material science applications. We are particularly interested in exploring the role of hysteresis, in this case the hysteresis in the modulus, as a function of effective pressure. Our interest in hysteresis arises from observations that indicate hysteresis is important in describing static and dynamic behavior in rocks. These results are based on static stress-strain results [e.g., *Guyer et al.*, 1994, 1995], propagating wave experiments at ambient conditions and under vacuum conditions [e.g., *Meegan et al.*, 1993; *Ten Cate et al.*, 1996; *Van Den Abeele*, 1996], and resonant bar experiments [*Kadish et al.*, 1996; *Johnson et al.*, 1996] in a variety of rocks under a variety of physical conditions (for a review of laboratory observations see *Johnson and Rasolofosaon* [1996b]).

In this work we explore the effect of increasing effective pressure on the nonlinear response of the material in terms of the behavior of resonant frequency shift with acceleration and harmonic response. We show that as the rock is pressurized and low aspect ratio pores close the nonlinear response of the rock progressively responds more and more as an intact solid (solid without low aspect ratio pores). We also show that the modulus in hysteric in these experiments.

We compare three very different rock types: A clean quartz sandstone (Fontainebleau sandstone), a sandstone containing clay (Meule sandstone), and a peletoidal limestone (Lavoux limestone) [*Lucet et al.*, 1991]. Pressure and water saturation results were compared to results obtained from two relatively elastically linear, intact standards: polycarbonate and Pyrex glass. A tangential goal was methodology development. That is, varying the effective pressure and therefore the elastic properties without change in the experimental apparatus is a unique approach to test nonlinear response and especially the delicate problem of harmonic measurement.

Experimental Configuration and Methodology

The resonant bar pressure vessel described by *Lucet et al.* [1991] is illustrated in Figure 1, and the experimental configuration is illustrated in Figure 2. The pressure apparatus in Figure 1 is designed to apply effective pressure to rock samples.

[1]Also at Laboratoire d'Acoustique Physique, Université Pierre et Marie Curie, Paris.

Paper number 96JB03225.
0148-0227/97/96JB-03225$09.00

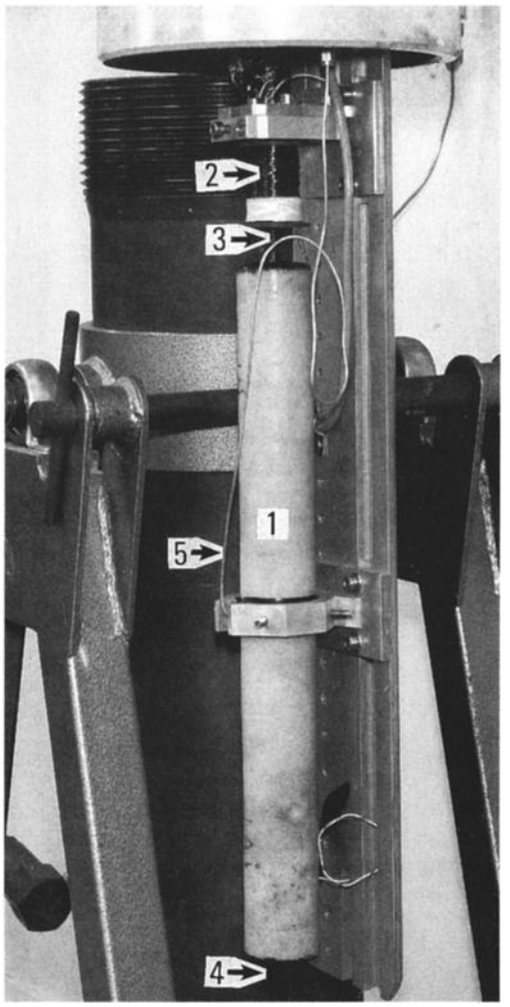

Figure 1. Photograph of effective pressure vessel. Numbers in photograph correspond to the following components: 1, jacketed sample; 2, coil; 3, magnet; 4, accelerometer; and 5, pore pressure tubing.

Effective pressure is the confining pressure minus the pore pressure. In order to perform measurements under effective pressure, the bar is jacketed using impermeable heat shrink tubing, and the ends of the samples are sealed with epoxy. A small stainless steel tube (component 5 in Figure 1) is placed in a hole drilled in the rod center, enabling control of the pore pressure while the rock is exposed to confining pressure applied by helium gas. In the experiments described here the pore pressure was kept at atmospheric pressure. As is standard in this type of experiment, the bar is clamped in the center to avoid clamping effects on the fundamental resonant mode.

The waveform excited by the source in the bar is the fundamental Young's (extensional) resonant mode. The resonance excitation and detection is described as follows. Following the block diagram in Figure 2, a function generator delivers a sinusoidal current of variable frequency and intensity through a high-power audio amplifier to a coil/magnet source (in Figure 1, component 2 shows the coil and component 3 shows the magnet). The source has been slightly modified from that described by *Lucet et al.* [1991]. The excitation coil and magnet have been altered in order to provide larger excitation intensities so that a larger interval in strain amplitude could be explored. The force transmitted to the bar is linearly proportional to the intensity of the current fed to the coil. For linear measurements the intensity is small and is therefore not an important experimental consideration; however, for nonlinear experiments the intensity is a consideration and will be addressed later in the text. The resonance waveforms are detected by a calibrated accelerometer attached at one end of the bar (component 4 in Figure 1). The signal is preamplified, time averaged in a voltmeter, and plotted versus frequency. In addition, the detected wave is directed to a digital oscilloscope for waveform harmonic analysis.

The frequency range of our experiments is controlled by bar lengths and fundamental Young's mode bar velocities. The dimensions of the rock samples and standards are 37 cm in length by 4 cm in diameter (see Table 1). The small mass loading effects of the source [*Lucet et al.*, 1991] are not accounted for because we are studying relative, not absolute, changes. Measurements are made of both upward and downward frequency sweeps over the chosen interval. Typically, 5–20 frequency sweeps are conducted at successively increasing drive excitation levels over the same frequency interval in order to monitor resonant peak shift and harmonic generation at a given pressure. A single frequency sweep is several minutes in duration.

The samples were studied in two states of fluid saturation. First, measurements were made in the dry state (air saturated) after oven drying at 70°C. Measurements were also made at near 100% tap water saturation. Water saturation was obtained from oven drying the samples under vacuum and then saturating the samples. (Note that it is well known that water saturation of 0% cannot be attained with oven drying at such temperatures and that water saturations of 100% are equally difficult to attain. also, it should be noted that water saturation is rarely uniform in rock, especially at intermediate saturation levels. Inhomogeneous water saturation will affect the nonlinear response of the materials to some degree but does not affect the general conclusions presented here.)

Studied Parameters and Measurement Accuracy

We employed a variety of approaches to be certain that the apparatus was operating as expected and not providing additional nonlinearities that may be mistaken for those generated in the rock, especially harmonics. In the following section we describe these tests and their implications.

Intensity and Q

In the "linear" elastic domain Q remains unchanged as a function of excitation intensity; however, we know from expe-

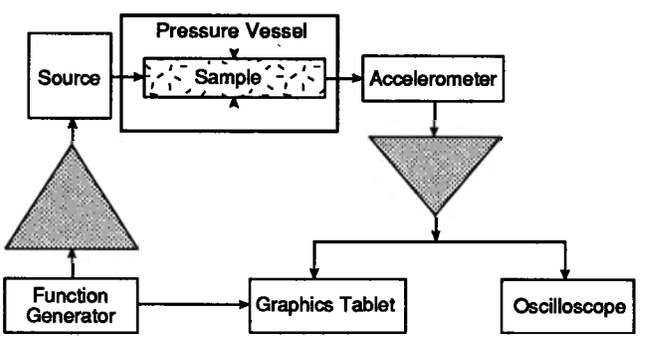

Figure 2. Block diagram of setup.

Table 1. Rock Physical Properties

Rock	Porosity, %	Air Permeability, mdarcy	Compressive Strength, MPa	Rock Type	Comments
Fontainebleau sandstone	17.1	1200	>70	pure quartz sandstone	extraordinarily sensitive to effective pressure, not representative of most sandstones
Meule sandstone	22.1	180	35	fine grained, argillaceous (Illite, Kaolinite) micaceous sandstone	probably representative of many sandstones
Lavoux limestone	23	6	~25	peletoidal limestone	probably representative of porous limestones

rience and the work of others [e.g., *Winkler et al.*, 1979; *Murphy*, 1982; *Johnson et al.*, 1996] that one must be careful in measurements of linear Q so as not to contaminate the result with nonlinear elastic effects of the rock or nonlinear instrumental effects. Figure 3 illustrates the relationship between the ratio of excitation intensity/detected acceleration measured at resonance, versus Q for the three rocks studied, dry and saturated. The data represent all effective pressure levels, and this is the reason for the variation for an individual rock under a particular dry/saturation condition. We note several observations from this plot. First, it is clear that we can predict Q at any excitation level from all rocks in saturated or dry conditions by measuring the ratio of excitation intensity/detected acceleration. Second, it is clear that for several of the experiments conducted on dry Lavoux sandstone, the measurements fall off the observed trend. We have evidence that the source magnet was depolarized from prolonged use and the consequent heating in these experiments. These data (including the measurements of the respective harmonic response and resonant frequency shift carried out simultaneously) were rejected. In addition, for the saturated sandstones at low effective pressures, Q can be less than 10. When Q is low, the resonant peak is very difficult to measure without error because the peak is very wide [*Johnson et al.*, 1996]. Saturated Fontainebleau and Meule sandstone exhibit low Q values. The accuracy on measured resonant frequency (and therefore frequency shift) for high-Q materials is much better than 1 Hz. On the other hand, for low-Q materials the resonance peak is so wide that only shifts of greater than 5 Hz could be detected. Several of the above points will be discussed further below.

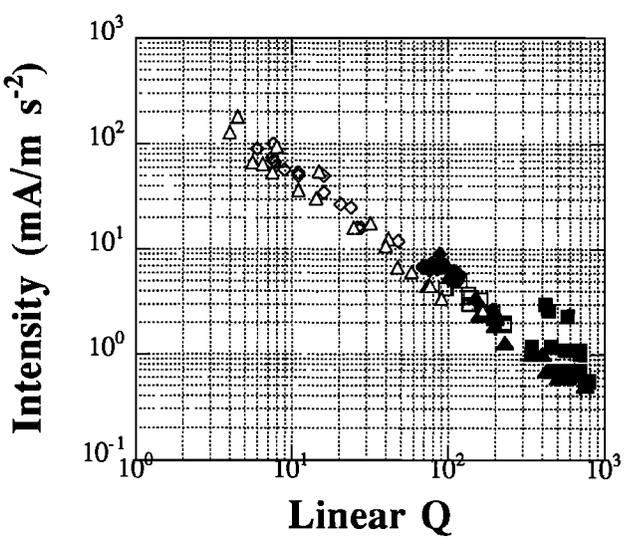

Figure 3. Normalized excitation intensity (measured at the source)/acceleration (measured at the detector) and Q for three rocks under saturated and dry conditions in the elastically "linear" domain. Data were taken at many effective pressures. The accuracy of measured resonant frequency (and therefore frequency shift) for high-Q materials is much better than 1 Hz; for low-Q materials the accuracy is 5 Hz. The precision is less than 1 Hz in all cases. Solid square, Lavoux dry; open square, Lavoux saturated; solid diamond, Meule dry; open diamond, Meule saturated; solid triangle, Fontainebleau dry; open triangle, Fontainebleau saturated.

Excitation, Resonant Frequency Shift, and Harmonics Versus Strain Level

In the following figures we illustrate three indicators of elastic nonlinear response: source excitation, resonant frequency shift, and harmonic generation. Figure 4 illustrates observations for dry Fontainebleau sandstone at increasing effective pressure levels up to 5 MPa, and at 1 MPa for decreasing pressure. In Figure 4a strain (calculated from detected acceleration [see *Johnson et al.*, 1996]) is plotted against the ratio of intensity/acceleration recorded at the resonant peak. Figure 4b illustrates strain versus normalized resonant frequency shift over the same pressure interval for this rock. The normalized resonant frequency shift $\Delta\omega = |\omega - \omega_0|$ where ω corresponds to the resonant peak as the peak shifts downward and ω_0 is the linear resonant peak. The third harmonic observations $\ddot{u}3/\ddot{u}1$ (measured acceleration of the third harmonic/fundamental frequency acceleration) are illustrated in Figure 4c. As noted by *Johnson et al.* [1996], there is a correlation in slope change between the excitation versus strain, the resonant frequency versus strain, and harmonic level versus strain. The slope change occurs at roughly 10^{-6} strain level (depending on the effective pressure level).

Resonant frequency shift never occurs in the intact standards we have investigated [*Johnson et al.*, 1996]; however, harmonics were observed during such experiments. Harmonics can potentially be generated in associated electronics, in the detectors, from the clamping, and jacketing of the sample in the vessel. Hysteretic behavior in the coil/magnet source generates harmonics as well. Because of the possibility of externally generated harmonics, we chose a pragmatic approach to the general problem. We measure nonlinear response from all external causes in the standards, over the same strain/excitation and pressure intervals as those for the rocks. We then have a baseline above which we trust the harmonic results. Below the baseline the results are disregarded.

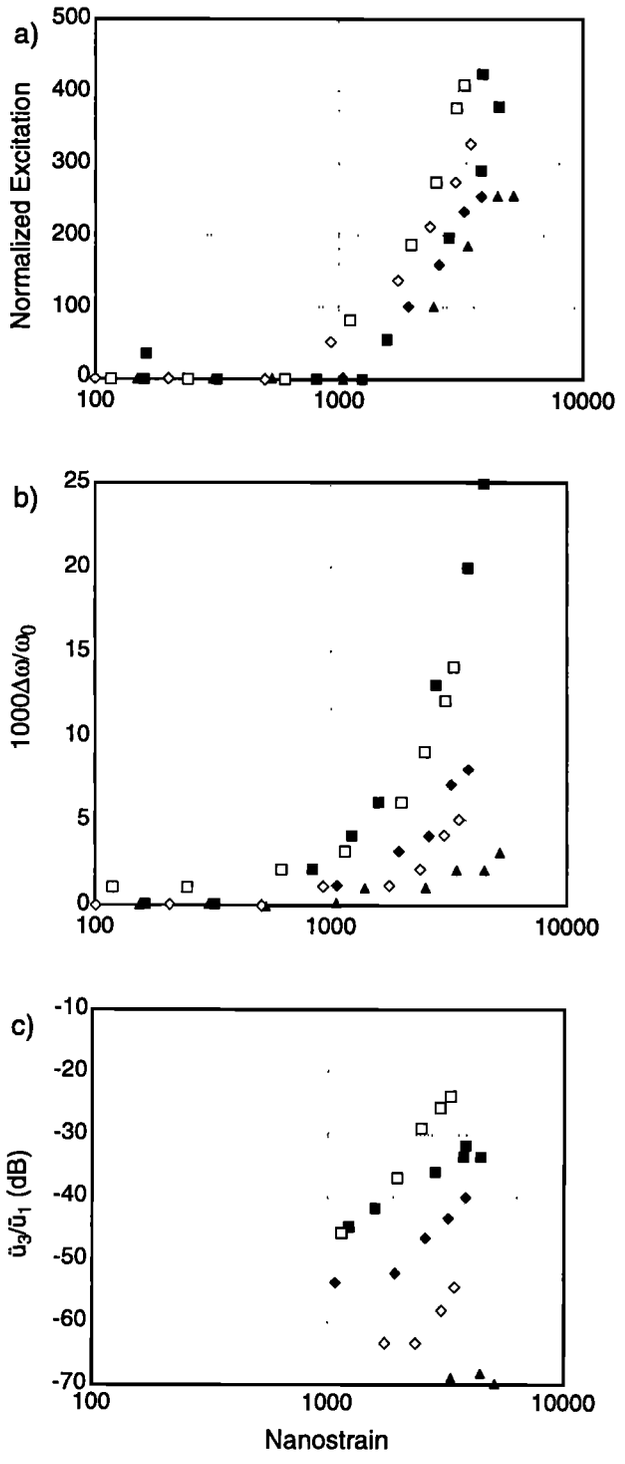

Figure 4. (a) Normalized excitation intensity (measured at the source)/acceleration (measured at the detector) versus dynamic strain for the five pressure levels indicated on the plot for dry Fontainebleau sandstone. The excitation intensity/acceleration ratio, measured in mA/m s^{-2}, has been normalized to the initial values in each case. (b) Normalized change in resonant frequency $|\Delta\omega/\omega_0|$ plotted against dynamic strain for the same sample. (c) Third harmonic level/fundamental ($\ddot{u}_3/\ddot{u}_1$) in decibels versus dynamic strain for the same sample. The accuracy of measured resonant frequency (and therefore frequency shift) for high-Q materials is much better than 1 Hz; for low-Q materials the accuracy is 5 Hz. The precision is less than 1 Hz in all cases. Solid square, 0 MPa; open square; 0.5 MPa; solid diamond, 1 MPa; open diamond, 2 MPa; solid triangle, 5 MPa.

The shape of the resonant frequency peak varies with the direction of driving frequency in the experiment. That is, one obtains a different shape for the resonance curve depending on frequency sweep direction, upward or downward. This was discussed by *Johnson et al.* [1996]. In this work we illustrate resonant frequency shift as a function only of increasing drive frequency.

Frequency sweep rate definitely affects the resonant peak and the general shape of the resonant peak curve for nonlinear materials, especially if the experiment is conducted very quickly [see *Ten Cate and Shankland*, 1996]. This is handled empirically by conducting all sweeps shown in this work at approximately the identical rate of several minutes per sweep.

Sensitivity of Nonlinear Indicators

The nonlinear indicators, harmonic generation, or resonant peak shift do not necessarily have the same measurement sensitivity. The sensitivity of each method is based in part on the sensitivity of measurement ability. For the resonant frequency shift measurement we can measure one part in several thousand at best. For harmonics we can measure better than one part in a thousand; however, it is straightforward to attain measurements of one part in 6.5×10^4 for the harmonic amplitudes by use of a 16 bit digitizer. Making the same improvement in the frequency shift measurement is currently not possible. Therefore, based on equipment arguments, harmonic generation is the most sensitive measure of dynamic nonlinear response if a 16 bit digitizer is used. In addition, it was shown by *Johnson et al.* [1996] that in some cases harmonic generation exists in the absence of resonant peak bending (e.g., chalk). It is therefore wise to always monitor harmonics in nonlinear experiments.

Slow Time Constant Effects

There are several slow time constant effects in our experiments that exist in both static and dynamic measurements. These effects are another manifestation of nonlinear response that may or may not be independent of resonant peak shift and harmonic generation. For example, we have discovered that a rock sample must be "conditioned" by sweeping at relatively large amplitude several times before the acceleration response is repeatable to 100% precision. The conditioned state was always attained before data were collected for the results presented here. Further, it may take seconds, minutes, or even tens of minutes for the linear resonant peak to match before and after a large-excitation frequency sweep. In this work the linear resonance peak was always monitored before and after large-excitation sweeps to be certain no permanent change took place in the rocks. These slow time constant effects are described by *Ten Cate and Shankland* [1996] and *Shamina et al.* [1990] and will not be discussed here. Another slow time constant effect exists upon effective pressure increases. After an increase the resonant frequency drifts for some time until it settles, and therefore it is necessary to wait for the frequency to stabilize at pressure. The measurements presented here were obtained after stabilization in all cases.

Measurements on Standards

Calibration experiments on polycarbonate ($Q = 100$) and Pyrex glass ($Q = 2000$) were performed over the same pressure range as that used in the testing of the rocks. Instrumental harmonic generation (distortion) due to associated electronics, the source, and the acceleration measurement device were

determined from these experiments. We know from previous experiments at ambient conditions that harmonic generation in glass is very small even at strain levels of 10^{-6}–10^{-5}. Inside the pressure vessel the harmonic ratios $\ddot{u}_3/\ddot{u}_1$ and $\ddot{u}_2/\ddot{u}_1$ versus acceleration measured at the fundamental $\ddot{u}1$ shown in Figure 5 exhibit a certain amount of second harmonic generation in experiments with glass. Note that there is no harmonic generation above the −50 dB level for accelerations lower than 400 m s^{-2}. During our experiments on rock this acceleration corresponds to the upper limit that we were able to reach. Thus from a practical point of view the instrumental/source/detector distortion is not a limitation. It could, however, become a significant problem if we were to modify our excitation device to reach much greater strain levels.

Figures 6a and 6b shows results of harmonic ratio $\ddot{u}_n/\ddot{u}_1$ (n = 2–5) versus detected strain level at the fundamental frequency for polycarbonate and Pyrex glass at 1 atmosphere confining pressure (note that we carefully checked to be certain confining pressure had no effect on the standards up to 45 MPa). We observe that the second harmonic is always the largest, and the remaining harmonics, if observed, are near or below 60 dB. We have never observed domination of odd harmonic amplitudes in the standards, nor are we aware of any such results; however, rock frequency exhibits domination of odd harmonic amplitudes. Based on these plots we delineate the area in Figures 6a and 6b in which we will use data obtained from the rock samples. The area, obtained empirically, is on the left side of the dashed line joining the strain/ratio points at 10^{-6}/−70 dB and 10^{-5}/−30 dB in the figures.

We do not have standards with the low-Q values observed for saturated rock samples (<10). This is a problem in testing the effect of the drive excitation on harmonic generation from the source, in particular. We are most suspicious of the source because of the results illustrated in Figure 3 that indicated magnet depolarization. We can, however, study the results of Fontainebleau sandstone, for which Q varies radically with water saturation and pressure. Figure 7 illustrates the results of

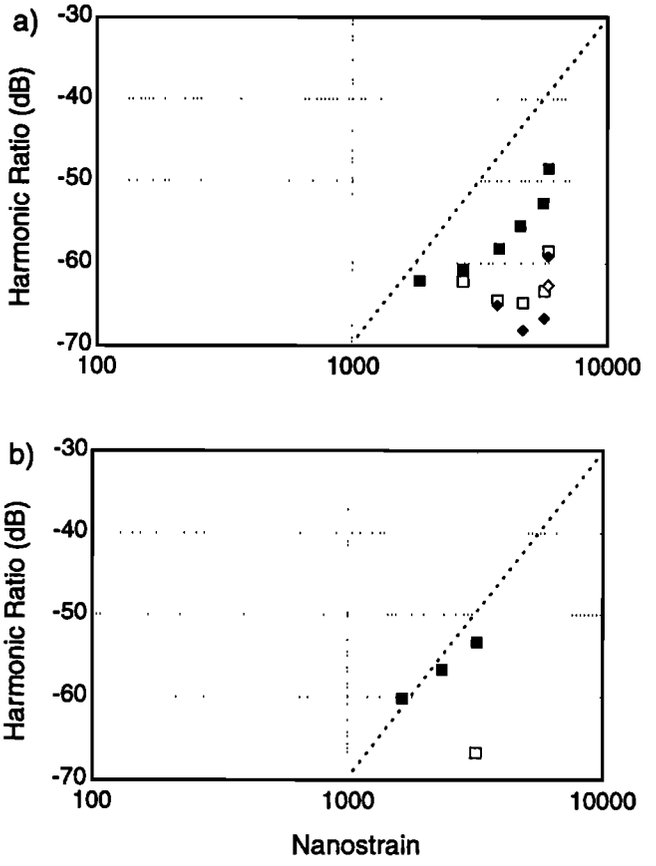

Figure 6. (a) Harmonic ratio versus dynamic strain in polycarbonate at 0 effective pressure (1 atmosphere confining pressure). (b) Same result for Pyrex glass. Dashed line indicates empirical base above which we trust the observations in rock. Each harmonic is normalized to the fundamental frequency amplitude ($\ddot{u}_1$). Solid square, $\ddot{u}_2/\ddot{u}_1$; open square, $\ddot{u}_3/\ddot{u}_1$; solid diamond, $\ddot{u}_4/\ddot{u}_1$; open diamond, $\ddot{u}_5/\ddot{u}_1$.

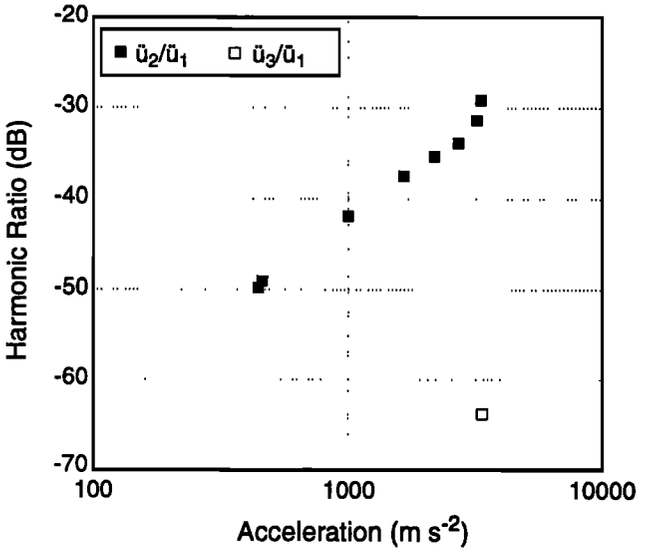

Figure 5. Instrumental harmonic generation in Pyrex glass primarily due to distortion in the accelerometric system: harmonic ratio of the second ($\ddot{u}_2/\ddot{u}_1$) and third ($\ddot{u}_3/\ddot{u}_1$) harmonics in decibels versus acceleration, in m s^{-2}. Note only one second harmonic was observed over this interval.

harmonic ratio for the second harmonic $\ddot{u}_2/\ddot{u}_1$ and third harmonic $\ddot{u}_3/\ddot{u}_1$ versus excitation intensity, obtained at all effective pressures measured from dry and saturated Fontainebleau. The observations of the second harmonic ratio (Figure 7a) indicate that there is not a large second harmonic ratio and that there is a tendency for the ratio to increase with intensity, despite a Q which ranges from 5 to 800. We therefore infer that the second harmonic could be of instrumental origin. The third harmonic (Figure 7b) has no clear relation with excitation intensity. For example, we observe a large third harmonic at low intensity and a very low ratio at high intensity. This observation suggests that the large third harmonic is not instrument related but instead related to the nonlinear response of the rock.

We therefore reach the following conclusions regarding the reliability of harmonic measurements. (1) Our instrumental noise level is about 60 dB; (2) at the strain levels in the standards corresponding to those observed in the rocks there is no noticeable instrumental third and higher odd harmonic generation; (3) however, we must be very careful in interpreting observations of second harmonic generation in the rock samples, especially samples with low Q (pressure unconfined). The accuracy and precision of the harmonic measurements is plus or minus several percent.

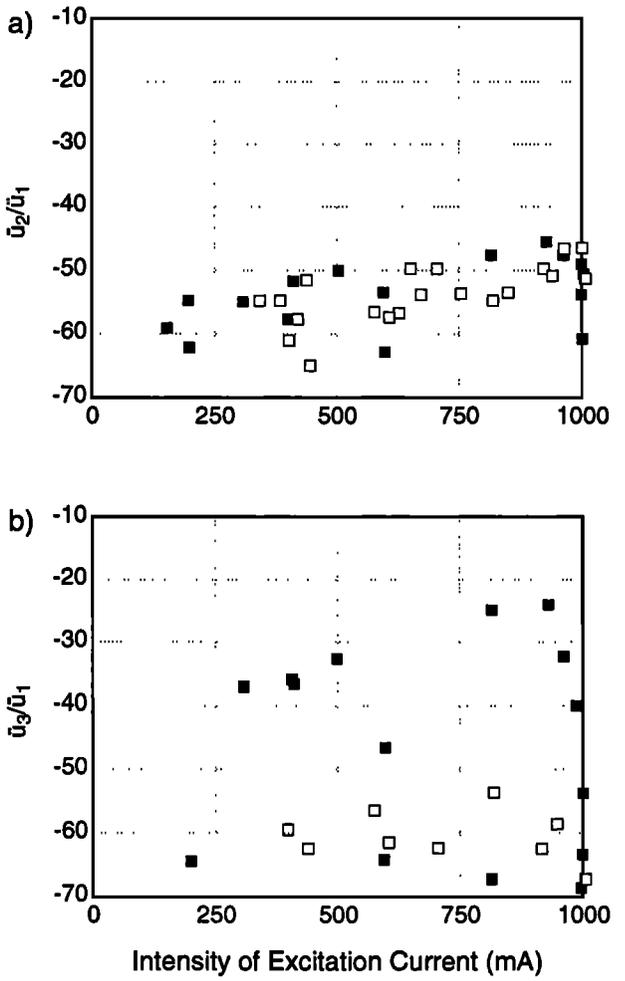

Figure 7. (a) Harmonic ratio of second harmonic versus excitation intensity in dry and saturated Fontainebleau sandstone. (b) Same plot for third harmonic. Each harmonic is normalized to the fundamental frequency amplitude ($\ddot{u}_1$). Solid square, dry; open square, water saturated.

Experimental Results on Rock

Extensional Velocity and Q as Functions of Effective Pressure

We focus our discussion in this section on the three types of sedimentary rocks described in the introduction, contrasting the evolution of extensional velocity and Q as a function of effective pressure. Figures 8a and 8b illustrate the behavior of the velocity and attenuation ($1/Q$) between the different samples in their dry and saturated states for upgoing pressure only. Pressure hysteresis observations will be illustrated in the following section. Tables 1 and 2 describe physical properties of the samples and Figure 9 shows thin section photos of the two sandstones and epoxy pore casts of the Fontainebleau sandstone and Lavoux limestones samples. The following general comments about the rocks are based on the information presented in Table 1, Figure 8a, 8b, and 9. (Further details regarding Table 2 will be discussed later.)

Fontainebleau sandstone. This rock is exceptional in its extreme reaction to pressure in both its velocity and Q response and in its relatively insensitive reaction of velocity to water saturation. The attenuation, on the other hand, is extremely sensitive to saturation. At pressures greater than 20 MPa the material velocity and attenuation respond to pressure increases much like an intact solid. Fontainebleau exhibits a composition (pure quartz) and pressure behavior (highly nonlinear with respect to pressure) that are extreme and not representative of most sandstones.

Meule sandstone. This sandstone is very sensitive to effective pressure as well, but less so than Fontainebleau. Unlike Fontainebleau, its velocity is sensitive to water saturation. Its attenuation behavior resembles Fontainebleau but is less extreme. This rock contains clay (Illite and Kaolinite) and micaceous material, unlike Fontainebleau, and is representative of a greater number of sandstones. At pressures greater than 20

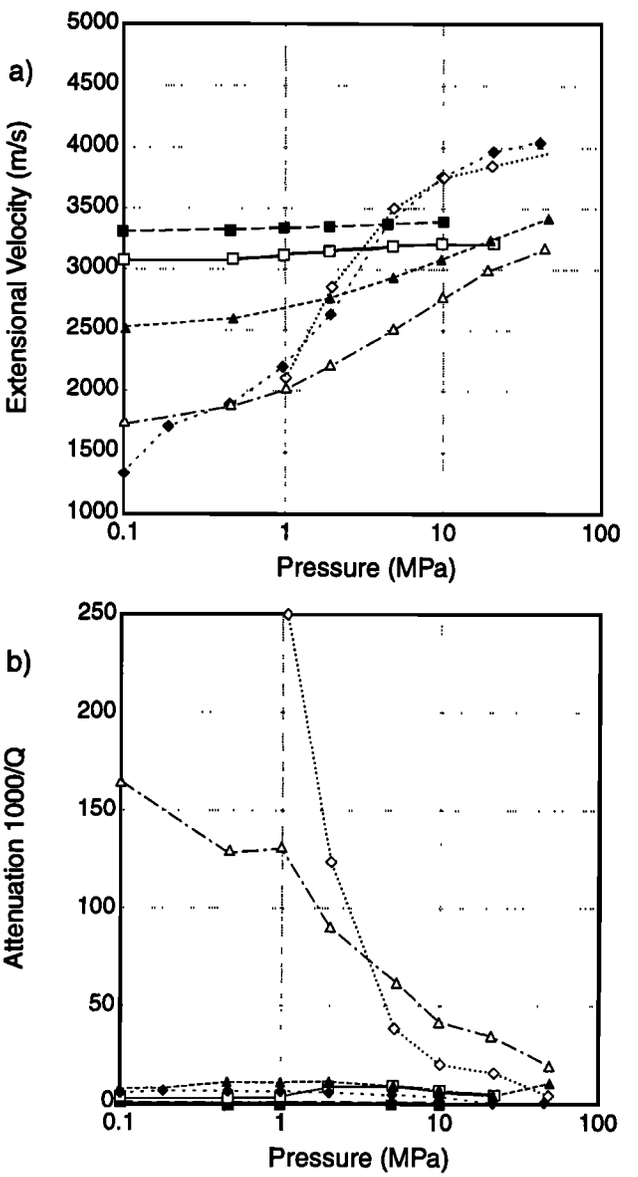

Figure 8. (a) Extensional velocity versus effective pressure in all three samples in their dry and water-saturated states (confining pressure equals effective pressure in this case). Increasing pressure curves only. (b) Same results for $1/Q$. Curves with solid square, dry Lavoux; open square, saturated Lavoux; solid diamond, dry Fontainebleau, open diamond, saturated Fontainebleau; solid triangle, dry Meule; open triangle, saturated Meule.

Table 2. Summary of the Variations of Linear and Nonlinear Elastic Response With Effective Pressure

	Linear and Experimental Parameters			Nonlinear Response			
				Frequency Shift			
	V_E, m/s	Q_E	Maximum Strain	Strain at Minimum Frequency Shift	Slope of $\Delta\omega/\omega_0$	$\Delta\omega/\omega_0$ at $\varepsilon = 3 \times 10^{-6}$ ($\times 10^3$)	Harmonic Generation
Low Effective Pressure (0–0.5 MPa)							
Fontainebleau sandstone							
Dry	1600	100	3×10^{-6}	10^{-7}	1.5	10	strong third and fifth harmonics
Saturated	NM	NM	NM	NM	NM	NM	
Meule sandstone							
Dry	2500	70	5×10^{-6}	10^{-6}	2	1.5	traces of third; second unreliable
Saturated	1800	6	10^{-6}	NM	NM	NM	second unreliable; traces of third and fourth
Lavoux limestone							
Dry	3300	500	10^{-5}	2×10^{-6}	1.5	0.5	moderate third; detectable fifth
Saturated							
Run 1	3100	150	5×10^{-6}	2×10^{-6}	2	2	rich harmonic content
Run 2	3000	150	5×10^{-6}	10^{-6}	1.4	4	rich harmonic content
Medium Effective Pressure (0.5–5 MPa)							
Fontainebleau sandstone							
Dry	2500	150	4×10^{-6}	10^{-6} to 2×10^{-6}	1.5 to>2	3	strong decrease of harmonics with pressure
Saturated	2500	10	3×10^{-7}	ND	ND	ND	significant third; second unreliable
Meule sandstone							
Dry	2900	100	3×10^{-6}	3×10^{-6}	2	0.5	traces of third; second unreliable
Saturated	2800	20	10^{-6}	ND	ND	ND	second unreliable; traces of third and fourth
Lavoux limestone							
Dry	3350	600	10^{-5}	3×10^{-6}	1.8	ND	rich harmonic content varying strongly but reproducible with pressure
Saturated							
Run 1	3200	150	5×10^{-6}	2×10^{-6}	2.3	0.5	second and third at limit of detection level
Run 2	3000	150	5×10^{-6}	10^{-6}	1.7	1.5	traces of third; traces of fifth
High Effective Pressure (5–50 MPa)							
Fontainebleau sandstone							
Dry	3800	600	8×10^{-6}	...	...	0	below detection level
Saturated	3800	100	1.5×10^{-6}	...	...	0	possible trace of third
Meule sandstone							
Dry	3200	100	3×10^{-6}	...	...	0	limit of detection level; trace of third
Saturated	3000	25	1.5×10^{-6}	...	...	0	limit of detection level; trace of third
Lavoux limestone							
Dry*	3400	800	10^{-5}	6×10^{-6}	1.9	ND	limit of detection level; trace of third and fifth
Saturated†							
Run 1	3200	200	7×10^{-6}	4×10^{-6}	2.2	ND	limit of detection level
Run 2	NM	NM	NM	NM	NM	NM	

NM, not measurable; ND, not detectable.
*Not measurable above 10 MPa.
†Not measurable above 20 MPa.

MPa the material velocity and attenuation also respond to pressure increases much like an intact solid.

Lavoux limestone. This limestone is relatively insensitive to pressure in its velocity and attenuation response. The sample is sensitive to water saturation. Attenuation is low in all saturation states, but its structure is altered when submitted to even very low effective pressures, especially when water saturated. It is probably representative of porous limestones.

Hysteretic Behavior of Extensional Velocity and Q

All the rocks studied exhibit some degree of hysteretic behavior in linear extensional velocity and Q as a function of effective pressure. The next group of figures illustrates this behavior. Figures 10, 11, and 12 show results from Fontainebleau sandstone, Meule sandstone, and Lavoux limestone, respectively. These figures illustrate effective pressure response in velocity and Q for dry and saturated samples, respectively, measured at both increasing and decreasing pressure. Velocity was calculated from the measured linear resonant frequency at each pressure. The pressure was normally cycled several times in order to check whether or not damage was induced. When possible, both dry and saturated runs are shown on the same plot. In the case of Lavoux, three samples were tested, and

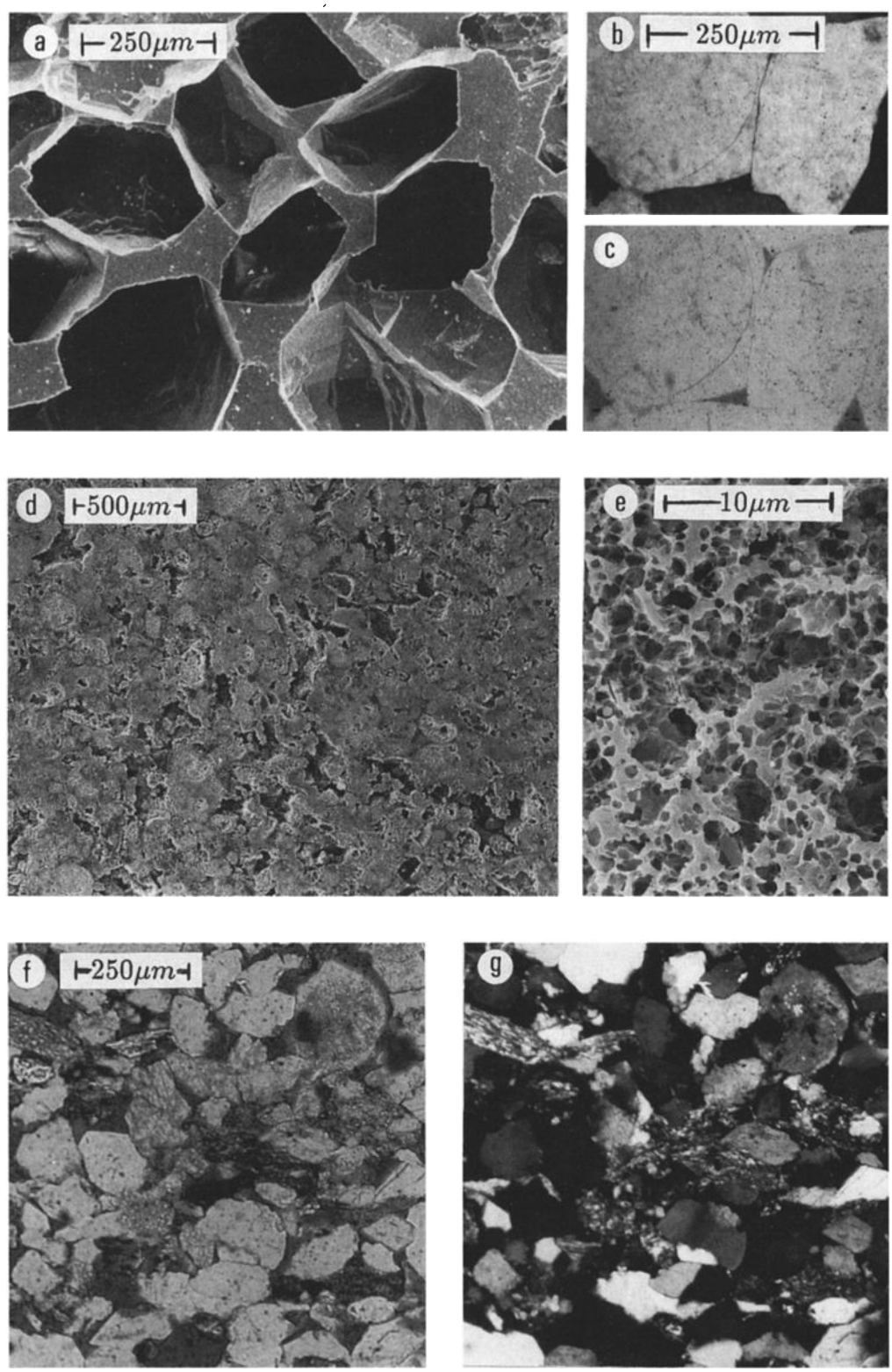

Figure 9. Thin section photographs and epoxy pore cast photographs of each of the three materials. The rocks include Fontainebleau sandstone, a rock that is composed entirely of quartz grains with syntaxic quartz cementation. The second rock studied was Meule sandstone, a quartz sandstone with notable clay and micaceous content. The grain cement is amorphous silica and clay. The third rock studied was Lavoux limestone, a peletoidal limestone bonded with microcrystalline calcite. For Fontainebleau sandstone, (a) epoxy pore cast, (b) thin section under polarized light, and (c) thin section under natural light (same scale as in Figures 9a and 9b) are shown. For Lavoux limestone, (d) epoxy pore cast and (e) epoxy pore cast under high magnification showing peletoidal structure are shown. For Meule sandstone, (f) thin section under natural light and (g) same section under polarized light are shown (same scale as Figure 9f).

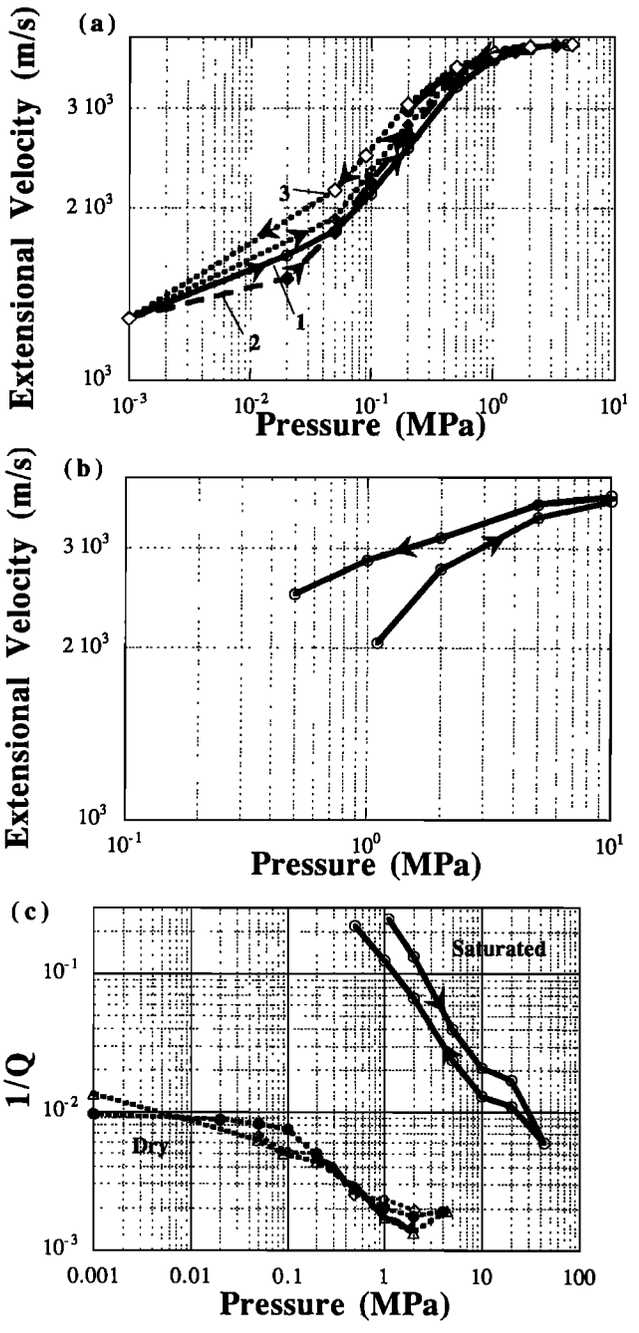

Figure 10. Effective pressure results for Fontainebleau sandstone. (a) Velocity versus effective pressure, dry sample, calculated from linear resonant frequency. Numbers 1, 2, 3 illustrate the order of pressure cycling. (b) Velocity versus effective pressure for the water-saturated sample. (c) Plot of $1/Q$ versus effective pressure, dry (dashed line) and water-saturated sample (solid line). Arrows indicate pressure direction, and actual data points are illustrated by solid and open diamonds. Precision and accuracy are within several percent after pressure cycling.

results from two are shown. The accuracy and precision in measurement of extensional velocity were described earlier. The accuracy and precision of the pressure response is within several percent once pressure cycling has taken place.

Fontainebleau sandstone. From the results on Fontainebleau sandstone in Figures 10a and 10b it is clear that velocity hysteresis exists to pressure at least 5 MPa in the dry sample and probably higher in the saturated sample. Otherwise, the dry and saturated responses are similar. We obtained measurements on the dry sample to considerably lower effective pressures because Q was larger. The Q response is seen in Figure 10c. Q ranges from roughly 100 to 800 in the dry case, and in the saturated case we observe hysteresis but only have reliable measurements between 1 and 40 MPa. Both Q and the velocity are larger in the downgoing portion of the cycle for both dry and saturated samples.

Meule sandstone. The velocity results in dry and saturated Meule sandstone illustrated in Figure 11a show that velocities are higher in the dry case, and velocity hysteresis exists to pressures of at least 10 MPa in the saturated state but not in the dry state. The Q shows no marked hysteretic effect in Figure 11b.

Lavoux limestone. An experiment on one sample of water saturated Lavoux limestone (not illustrated) showed long-term change in the sample velocity before and after a pressure excursion to 40 MPa. The change in resonant frequency (velocity) was enormous just after the pressure excursion. After several weeks, the velocity approached the prepressure-excursion velocity. We believe that this change could be related

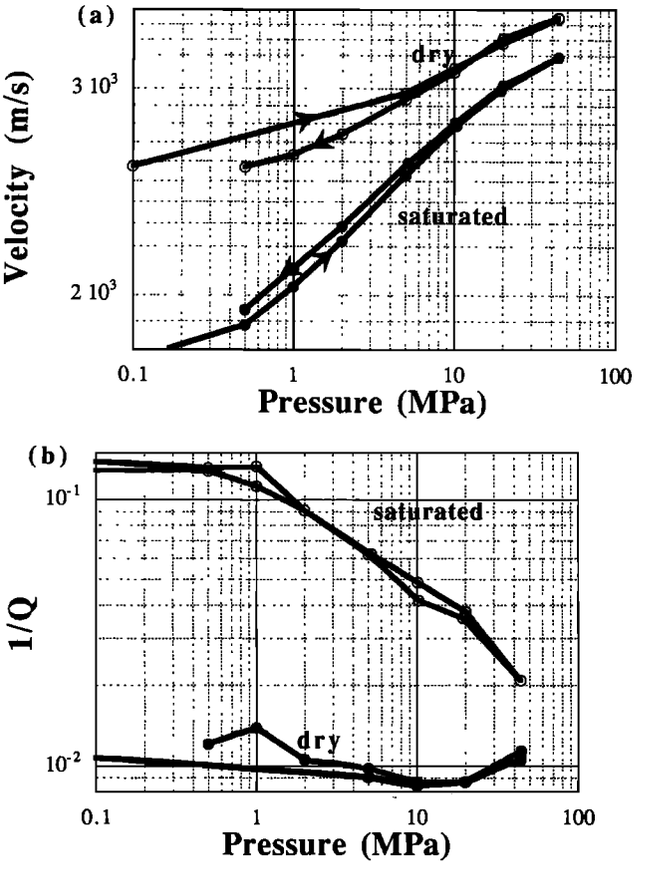

Figure 11. Effective pressure results obtained for Meule sandstone. (a) Velocity calculated from linear resonant frequency versus effective pressure, dry sample, and water-saturated sample. (b) Plot of $1/Q$ versus effective pressure, dry sample, and water-saturated sample. Arrows indicate pressure direction, and actual data points are illustrated by symbols. Precision and accuracy are within several percent after pressure cycling.

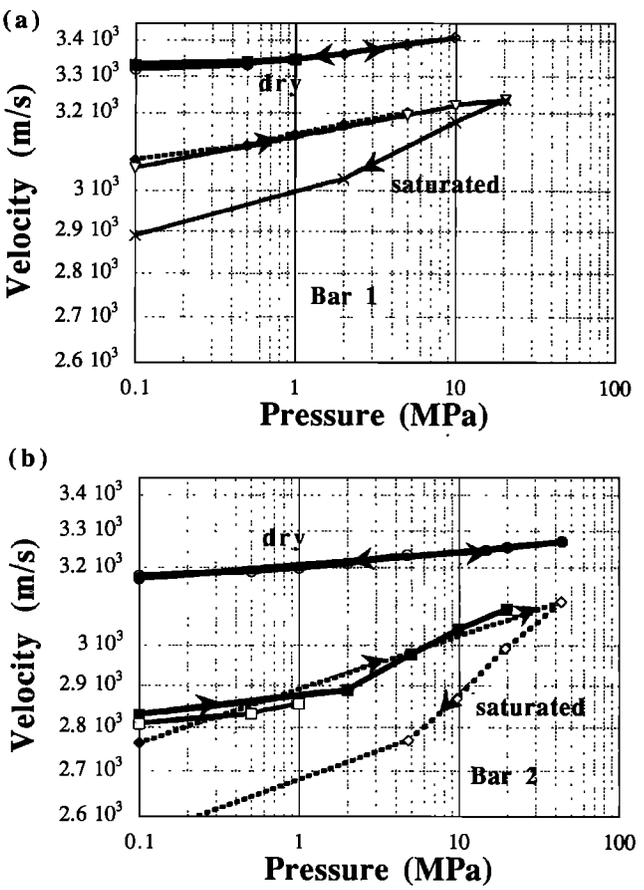

Figure 12. Effective pressure results obtained for Lavoux limestone. (a) Bar 1, velocity calculated from linear resonant frequency versus effective pressure, dry sample, and water-saturated sample. Dashed line shows second test. (b) Bar 2, velocity versus effective pressure, dry sample, and water-saturated sample; several runs in pressure. Arrows indicate pressure direction; actual data points are illustrated by symbols. Precision and accuracy are within several percent after pressure cycling.

to variations at calcite microcrystalline contacts. The extreme sensitivity of calcite to pressure is well known. We were therefore limited to maximum pressures of 10 MPa in effective pressure on the dry sample and 20 MPa for the saturated sample that are illustrated.

Figure 12 displays the results for Lavoux limestone. Lavoux limestone demonstrates a very different type of velocity hysteresis. Velocity hysteresis is observed in the saturated results as is illustrated in Figures 12a and 12b for the two different samples. (The Q results are not of good quality and are not shown.) No velocity hysteresis was observed over these intervals in the dry samples. Velocities were lower after the pressure excursion to >10 MPa.

Dynamic Nonlinear Elastic Response: Frequency Shift and Harmonic Response in Rock as Functions of Effective Pressure

Because we generally observe hysteresis in velocity and Q as functions of effective pressure, it comes as no surprise that the dynamic nonlinear indicators display hysteretic behavior as a function of effective pressure as well. At each effective pressure step shown in Figures 10–12 we also measured resonant frequency shift and harmonic generation as functions of excitation intensity and detected acceleration level. The results are summarized in Tables 2 and Figure 13.

In this section we focus on the evolution of dynamic nonlinear elastic response as a function of effective pressure. We will show that as effective pressure is increased, in general, the slope between frequency shift and strain in a log-log plot approaches 2, as is predicted by classical nonlinear theory. This result implies that with increasing effective pressure the materials begin to resemble nonhysteretic intact solids [see *Johnson et al.*, 1996]. This is important because it implies that classical nonlinear theory may be appropriate for rocks at high pressure. In addition, we observe a diminishing harmonic content that corresponds in a general manner to the evolution in the above slope.

Table 2 presents a summary of observations, separated into three pressure intervals that correspond to approximate slope changes in the frequency/strain relation illustrated in Figure 13. Primary column headings in Table 2 are divided into linear experimental parameters and nonlinear parameters, including resonant frequency shift and harmonic generation. The linear parameters include extensional velocity, extensional Q, and maximum strain levels attained. Under the nonlinear response-frequency shift heading, the strain observed at the minimum resonant peak shift, the slope of frequency shift, and the frequency shift at 3×10^{-6} strain are provided (the difference of the resonance frequency from its linear value [$\Delta\omega$] is normalized against the linear resonant frequency [$|\Delta\omega/\omega_0|$]). Notes of which harmonics were observed, if any, are provided under the nonlinear response heading. The notes on harmonics in the table correspond to the observations in Figure 13.

Examples of measurements of the resonance frequency versus strain are also shown in Figure 14 for dry Fontainebleau sandstone and saturated Lavoux limestone. In the figures, frequency change $\Delta\omega$ is again normalized against the linear resonant frequency ω_0. The slope approaches 2 in the dry sample as pressures increase to 5 MPa (Figure 14a). The saturated Lavoux limestone sample illustrates very different behavior (Figure 14b). The saturated Lavoux limestone, which exhibits a slope of more than 2 at 0 effective pressure, exhibits a slope of about 1.6 after pressure loading and unloading. We interpret this as manifestation of physical/chemical change.

The minimum strain at which resonant frequency shifts are detected can be 10^{-7} or less at low effective pressures (Table 2), for instance, in dry Fontainebleau sandstone, and this was noted previously in other rocks in resonance and pulse-mode studies [e.g., *Meegan et al.*, 1993]. In dry Fontainebleau, frequency begins to shift at strains of less than 10^{-7}, reconfirming that in some rocks at certain pressure and saturation states, there are clear manifestations of nonlinear elastic response at strains lower than is commonly appreciated. We also point out, however, that the same rock no longer shows resonant frequency shifts at a strain below 7×10^{-6} under moderate effective pressure (5 MPa).

In low-Q samples (low effective pressure, saturated sandstone) for which we were not able to excite strains greater than 10^{-6}, we observe third harmonics at strains as low as 5×10^{-7} (e.g., saturated Fontainebleau sandstone, Figure 13). In the sample of Meule sandstone we observe a very strong second harmonic (Figure 13) which is above the empirical cutoff.

Lavoux limestone, both dry or saturated, exhibits a rich harmonic spectrum (see Figure 13). This, in part, is related to the very low attenuation exhibited by this rock; because dissi-

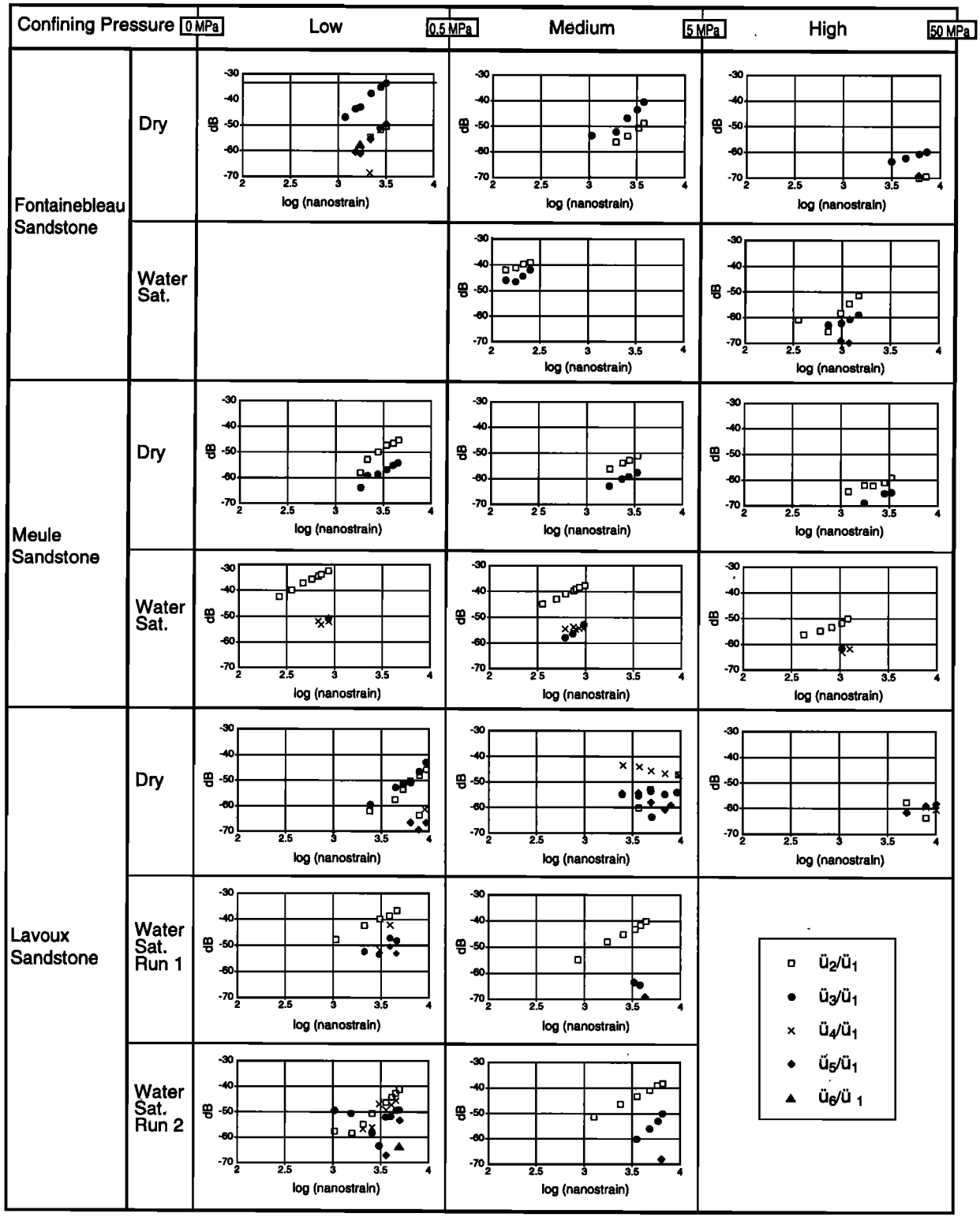

Figure 13. Harmonic observations at three effective pressures for dry and saturated samples of the three rock types. Harmonics illustrated are ratios of the $\ddot{u}_n$th harmonic acceleration amplitude to the fundamental where $n = 2, 3, 4, 5$. Harmonic data in the "low"-pressure region were taken at 0 effective pressure except for Meule sandstone (0.5 MPa). Those in the medium effective pressure level were taken at either 1 or 2 MPa. Those at high effective pressure were taken at between 5 and 20 MPa (confining pressure equals effective pressure in this case). The errors in harmonic amplitudes are less than 5%.

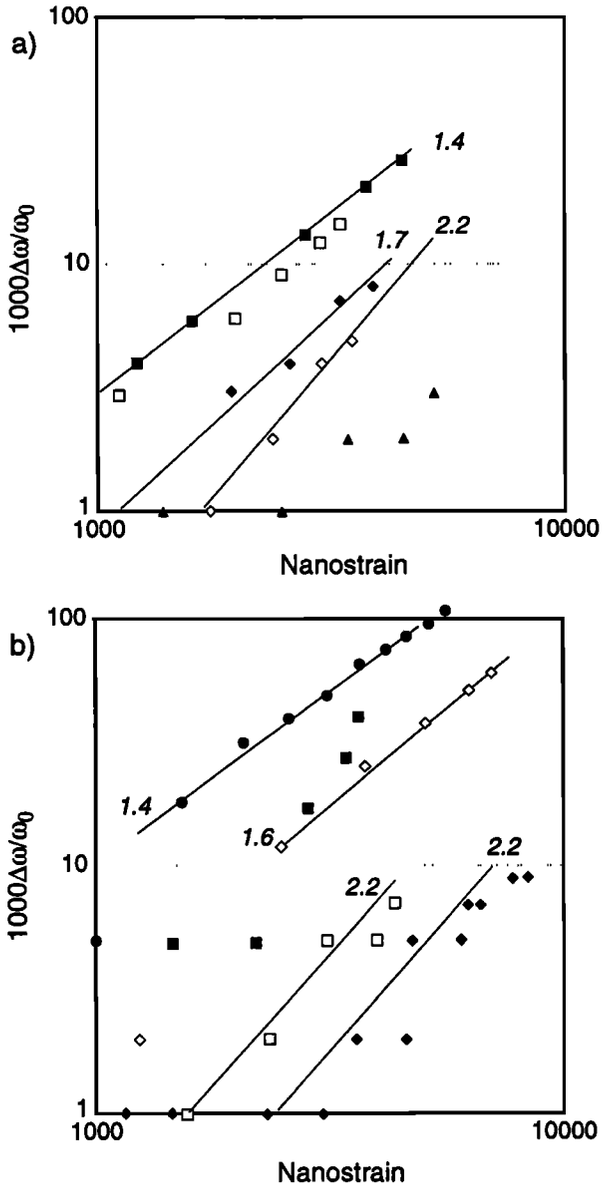

Figure 14. Sample dynamic strain versus frequency shift $|\Delta\omega/\omega_0| \times 10^3$ plotted in log-log space at the effective pressure noted in the legend for (a) dry Fontainebleau sandstone and (b) saturated Lavoux limestone. The numbers next to the various lines indicate the slope of the fits to each line. Errors in measurements are within approximately 1% in frequency ratio. For Figure 14a, solid square, 0 MPa; open square, 0.5 MPa; solid diamond, 1 MPa; open diamond, 2 MPa; solid triangle, 5 MPa. For Figure 14b, solid square, 0 MPa (initial); open square, 5 MPa (increasing pressure); solid diamond, 10 MPa; open diamond, 2 MPa (decreasing pressure); solid diamond, 0 MPa (final).

pation is low, harmonics are more easily measured. In addition, at roughly 1 MPa effective pressure, dry Lavoux exhibits a rich harmonic spectrum that is highly variable in relation to small effective pressure changes but is reproducible.

For sandstones under high effective pressure (Table 2), where no resonant frequency shift is detectable, harmonic analysis (Figure 13) shows traces of third harmonics above the limit of detectability of our system. Thus we have evidence of nonlinear elastic response at moderate strain level (3 to 7 × 10^{-6}) in some rocks under high effective pressure as well.

In order to compare frequency shift and harmonic generation for the three rocks as a function of effective pressure, we chose to present the results at a single measured strain value of

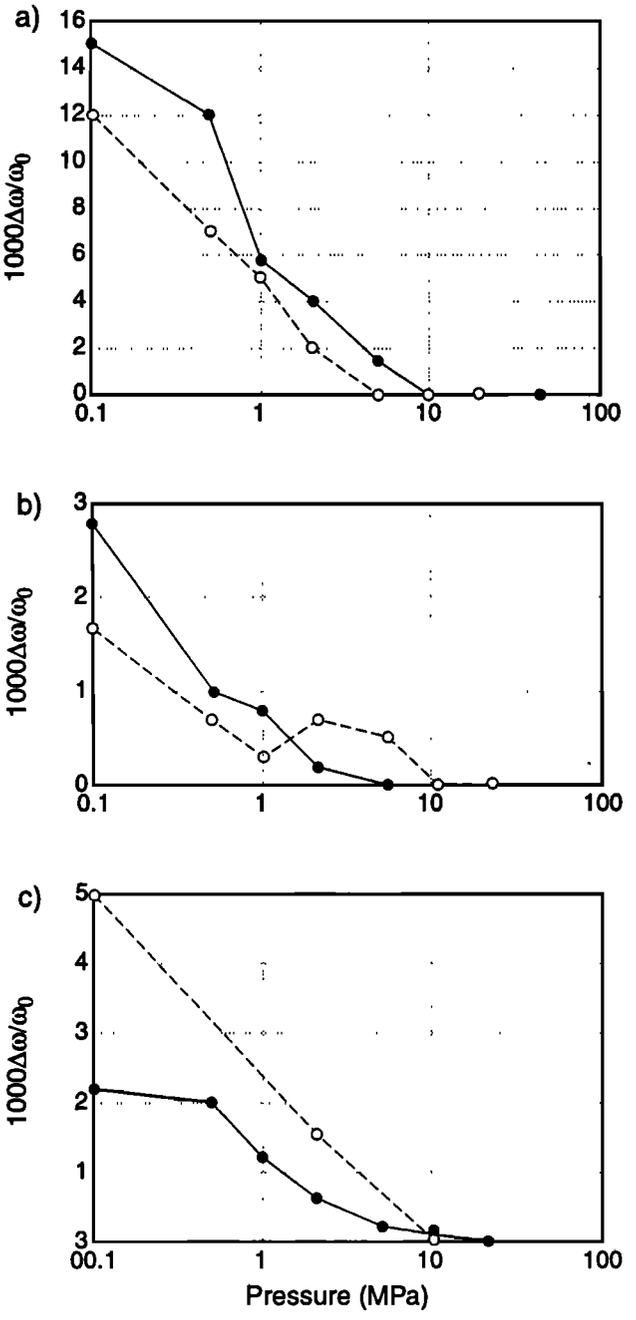

Figure 15. Hysteresis in resonant frequency shift as a function of pressure. Frequency shift ($|\Delta\omega/\omega_0| \times 10^3$) versus effective pressure (confining pressure equals effective pressure in this case) plotted at a constant dynamic strain level of 3×10^{-6} for (a) dry Fontainebleau sandstone, (b) dry Meule sandstone, and (c) saturated Lavoux limestone. Note the y axis scale is different in each case. Absolute measurements of frequency are within 1% here except in the region between 0 and 1 on the frequency scale. The pressure measurements are extremely accurate and repeatable. Solid circle, decreasing pressure; open circle, increasing pressure.

3×10^{-6} because of the difficulty in displaying the results as a function of dynamic strain (or acceleration). This is a convenient strain because it is the best represented value among the three rocks.

The results of the three rocks are illustrated in Figures 15a, 15b, and 15c and Table 2. Variable $|\Delta\omega/\omega_0|$ is plotted against effective pressure at the above strain level. The results for the two dry sandstones are shown along with the water saturated limestone results. Note that in each rock above 10 MPa, the resonant frequency no longer shifts at this strain. Note also that the results below 10 MPa are "hysteretic" as well, at least

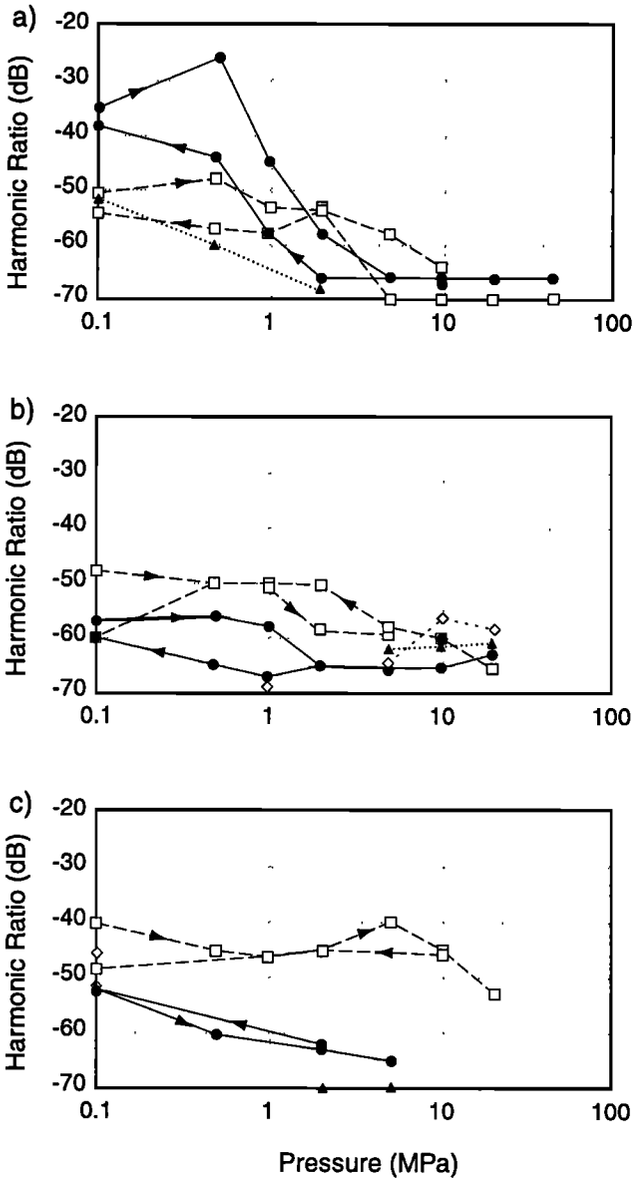

Figure 16. Hysteresis in the harmonic ratio as a function of pressure. Harmonic ratio in decibels versus effective pressure in mega pascals for harmonics. Variables $\ddot{u}_2$ through $\ddot{u}_5$ are plotted at a constant dynamic strain level of 3×10^{-6} for (a) dry Fontainebleau sandstone, (b) dry Meule sandstone, and (c) saturated Lavoux limestone. The errors in harmonic amplitudes are less than 5% (confining pressure equals effective pressure in this case). Each harmonic is normalized to the fundamental frequency amplitude ($\ddot{u}_1$). Curves with square, $\ddot{u}_2/\ddot{u}_1$; circle, $\ddot{u}_3/\ddot{u}_1$; diamond, $\ddot{u}_4/\ddot{u}_1$; triangle, $\ddot{u}_5/\ddot{u}_1$.

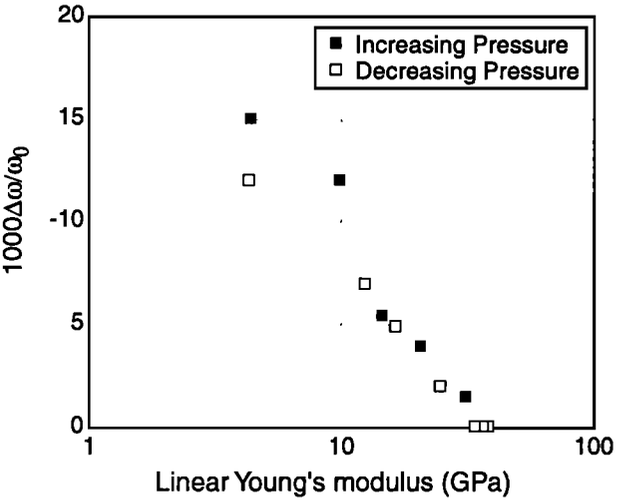

Figure 17. Young's modulus plotted against $|\Delta\omega/\omega_0| \times 10^3$ at a constant dynamic strain of 3×10^{-6} for dry Fontainebleau sandstone. Note that the hysteresis in the frequency shift approximately tracks the linear Young's modulus at this dynamic strain level. Errors in measurements are within approximately 1% in frequency ratio.

for the Fontainebleau and Lavoux samples. Increasing and decreasing pressure cause different amounts of frequency shift. In dry Meule and slopes actually cross one another, but note the frequency scale where this takes place: we are near our experimental resolution.

Figure 16 illustrates the results of comparing the harmonic ratio to effective pressure, taken again at the fixed dynamic strain value of 3×10^{-6}, for the three rocks in the same saturation states as those in Figure 15. The results approximately parallel those observed for the frequency shift results described above. In dry Fontainebleau sandstone, the harmonics are reliably observed to ~5 MPa. The third harmonic ratio is impressively large. Hysteresis in harmonic content is also observed at least in the Fontainebleau sandstone sample, and the results are in the same sense as those for frequency shift. That is, just as there was more resonant frequency shift for increasing pressure at this strain level, so to is there more harmonic generation, depending on the harmonic. This is best noted for the third harmonic in the Fontainebleau sandstone sample. It appears in the Meule sandstone sample for the third harmonic as well, but not in the Lavoux limestone. In the latter two rocks, harmonic generation is not reliably measured above 10 MPa. The second harmonic may be instrumental in origin in the two sandstones based on comparison with the standards. In the Lavoux limestone, the second harmonic dominates in amplitude and displays some hysteresis.

In summary, we see typical linear and nonlinear behavior of the samples when examined in response to effective pressure. The Fontainebleau sandstone is highly responsive to pressure, Meule sandstone is less so, and Lavoux limestone is far less so. Hysteresis in the modulus and Q are observed in the Fontainebleau sandstone and Lavoux limestone samples to at least 10 MPa in some saturation states. Long-term changes occurred in the modulus and Q for the Lavoux limestone. Observations of the dynamic, nonlinear elastic behavior show that the nonlinear indicators described here, resonant frequency shift and harmonic generation, can be hysteretic as well.

Discussion

Hysteresis in Nonlinear Indicators

For some of the samples, for instance Fontainebleau sandstone, we observe hysteresis in the modulus as a function of effective pressure, and hysteresis in the resonant frequency shift and harmonic generation. At a given pressure, nonlinear indicators (resonant peak shift and harmonics) are notably higher with increasing effective pressure when compared to the results at decreasing effective pressure for this rock. In some cases the hysteretic response of nonlinear indicators is linked to the hysteresis in the modulus. For example, if we plot Young's modulus (calculated from the linear response frequency) in place of pressure (Figure 17), the hysteresis in the resonant frequency shift disappears except at low modulus values. That is, the frequency shift at this strain approximately tracks the hysteresis in the modulus. This effect is also true for saturated Lavoux limestone; however, we also observe hysteresis in the modulus and no other little hysteresis in harmonic content (e.g., $\ddot{u}_3/\ddot{u}_1$ in saturated Lavoux), meaning that the phenomena can be independent.

Influence of Change in Physical State on Nonlinear Response

Influence of water saturation. In the sandstone studied here, particularly under low effective pressure, water saturation has an enormous effect on increasing attenuation. This is a very well known observation [e.g., *Lucet et al.*, 1991]. Consequently, experiments aimed at observation of nonlinear response are particularly difficult. With our experimental configuration we were unable to induce strains larger than 10^{-6} in saturated samples. For example, third harmonic generation in dry Fontainebleau sandstone is clearly observed to be much larger than in saturated Fontainebleau (Figures 7 and 16a). In general, it is clear from the results on the two sandstones that even at low strain amplitudes nonlinear response in terms of harmonic generation is larger in dry samples. This result deserves further study.

For the Lavoux limestone sample the results are markedly different. Because water saturation does not affect attenuation to the degree it does in the sandstone, we were able to perform measurements over a larger saturation/strain range. Water saturation increases resonance peak shift notably, and, to a lesser extent, harmonic generation.

Influence of effective pressure. Effective pressure has a large effect on the nonlinear response of all rocks studied. For the dry sandstone the resonant frequency shift is unmeasurable above roughly 10 MPa. In addition, this pressure corresponds roughly to the stabilization of the linear modulus and Q (much smaller pressure time relaxation constant).

The Fontainebleau sandstone sample exhibits an intense nonlinear response at low effective pressure. Odd harmonic generation is impressively large, as is the frequency shift; however, by 40 MPa effective pressure, Fontainebleau responds much like Pyrex glass. We attribute this behavior to the fact that this rock is a pure quartz sandstone with no clay and large numbers of low aspect ratio pores, as can be observed in Figure 9a. It is initially highly compressible as a result but responds like an intact solid when the grains contact.

For dry Meule sandstone, harmonic generation and frequency shift is less than that for Fontainebleau. We believe that the slow settling response is also longer because of the presence of clay.

In the Lavoux limestone we observe two contradictory trends. First, effective pressure reduces the nonlinear response notably; however, the effective pressure induces a modification of the rock microstructure leading to a subsequent increase in the nonlinear response, as seen best in the increase in harmonic response (see Figure 13) and resonant frequency change (Figure 14b) in the saturated state. We believe that this behavior is due to induced damage but not entirely in the common sense of the term, because we observe a certain amount of reversibility. We believe instead that the behavior may be in part due to the extreme sensitivity of calcite to physiochemical perturbation. That is, the grain bonding is altered, perhaps in addition to some microcracking. As it is very difficult to observe additional small amounts of microcracking in highly porous rock, we can only speculate.

Theoretical considerations. The general results regarding hysteresis of velocity (modulus) with effective pressure, and the results regarding the slope of the frequency shift versus strain as a function of pressure, are significant. The results indicate that because pressure hysteresis is present up to some effective pressure that is dependent on the rock type, classical nonlinear theory cannot be applied to rock. Above pressures where hysteresis is not apparent, classical theory may be appropriate.

The significance of the measured slope between frequency shift and strain during resonance is that it tends toward a value of 2 as pressure increases. This a fundamental prediction from classical theory. This result implies that with increasing effective pressure the materials begin to resemble nonhysteretic, intact solids [see *Johnson et al.*, 1996].

The classical nonlinear acoustics approach to describing static and dynamic nonlinear behavior involves expanding the modulus in Hooke's law as a power series in strain, and keeping one or two higher-order terms (e.g., $\sigma(\varepsilon) = \varepsilon(K + \beta\varepsilon + \delta\varepsilon^2 + \dots)$ where σ is stress, ε is strain, and β and δ are the nonlinear coefficients) [e.g., *Hamilton*, 1986; *Van Den Abeele*, 1996]. From this relation, static stress-strain observations can be described if hysteresis is not present or is ignored, and the relation can also be placed into the wave equation in order to describe propagating or resonant waves. Classical nonlinear theory for resonant behavior cannot be used to predict the behavior of material with hysteresis and discrete memory [*Guyer et al.*, 1995], because, as stated above, classical theory does not predict the slope changes between frequency and strain until pressure hysteresis disappears. In addition, harmonic amplitudes are not predicted well. This conclusion reinforces that of *Johnson et al.* [1996], *Van Den Abeele* [1996], *Guyer et al.* [1995, and references therein].

Static measurements have been described by a model containing hysteresis and discrete memory developed in a series of papers by *McCall and Guyer* [1994] and *Guyer et al.* [1994, 1995]. The method has had success in predicting dynamic behavior as a function of pressure, with some limitations [see *Van Den Abeele et al.*, 1997]. These authors are currently developing the model further for dynamic applications.

We have not discussed the effect of anisotropy on the measurements presented here. Anisotropy does influence all measurements described in this paper, but it was not the purpose of this work to investigate these effects. Some work has been conducted in this area [e.g., *Johnson and Rasolofosaon*, 1996b] and we intend to explore anisotropy and nonlinear response at pressure further in future studies.

Conclusions

The experimental setup is particularly convenient for nonlinear resonance measurements for medium- and high-Q rocks under effective pressures up to 50 MPa; resonant frequency shift is easily and accurately measurable and, using a pragmatic approach, we show that harmonic generation is reliably measured when dealing with odd harmonics. For even harmonics we suspect instrumental contributions dominate primarily at high excitation intensity.

For low-Q rocks (primarily saturated sandstones at low effective pressures) the measurements are much more difficult to interpret due to several problems. The very wide resonance peaks do not allow us to measure accurately the frequency shift, and we have found that the force necessary to maintain excitation in the strain range higher than 10^{-6} would necessitate a very high intensity current leading to demagnetization of the magnet and, moreover, to additional instrumental harmonic generation. We are currently circumventing this problem by the use of high-quality samarium-cobalt magnets.

In summary, we see typical behavior of the samples when examined in standard manners. The Fontainebleau sandstone is highly responsive to pressure, Meule sandstone is less so, and Lavoux limestone is far less so. Hysteresis in the modulus and Q are observed in the Fontainebleau and Lavoux samples to at least 10 MPa depending on saturation. Long-term changes occurred in the modulus and Q for the Lavoux limestone. Observations of the dynamic, nonlinear elastic behavior show that two of the nonlinear indicators described here, resonant frequency shift and harmonic generation, can be hysteretic as well. Effective pressure has a strong effect on the nonlinear response of all materials studied. For the dry sandstones the resonant frequency shift vanishes above roughly 10 MPa. In addition, this pressure corresponds roughly to the stabilization of the linear modulus and Q (much smaller time relaxation constant). It also corresponds to a general change in slope of the resonant frequency-strain relation. It is clear from the results on the two sandstones that even at low strain amplitudes nonlinear response in terms of harmonic generation is larger in dry samples.

The most important information derived from this study includes the observation that velocity and Q hysteresis can be present in these rock samples and that the hysteresis is unmeasurable above a certain effective pressure, depending on the rock type. Static tests have indicated this behavior in numerous rock types by many researchers over the past 50 years. This observation suggests that above the pressure when hysteresis disappears, classical nonlinear theory may be adequate; however, at lower pressures a theory containing hysteresis and discrete memory is absolutely necessary in order to correctly describe linear and nonlinear behavior of the rock. Pressure history is equally important. That is, in the simplest terms, one must be aware of whether a rock is measured after upgoing or downgoing pressure has been applied. This result clearly is important for core measurements where one is nearly always measuring properties of a sample after pressure release (excluding overpressured media). Slow time constant pressure relaxation is also an important parameter. That is, linear and nonlinear rock properties measured immediately after an effective pressure change (e.g., just after removal from the ground) can demonstrate far different behavior minutes or hours later. Clearly, in the case of core this argues for immediate field measurement or special handling. Taken in sum, the work presented here tells us that comparisons of linear and nonlinear properties between rock samples may be misleading unless much is known about the rock pressure history, pressure relaxation time constant, and time of measurement after pressure excursion. Further, extrapolating to in situ conditions should be approached with caution.

Hysteresis and other manifestations of nonlinear behavior (harmonics, resonant frequency shift) are related to compliant features in rock. Currently, we are studying precisely how they relate. We are addressing the issue of what practical applications can arise from study of nonlinear response of rocks and other materials.

Acknowledgments. This work was performed under the auspices of the Offices of Basic Energy Research, Engineering and Geoscience (contract W-7405-ENG-36), U.S. Department of Energy with the University of California, and the Institut Français du Pétrole. We thank Michel Masson for experimental assistance and thank Thomas Shankland and James Ten Cate for helpful discussions. We are indebted to Robert Guyer, Abraham Kadish, Katherine McCall, and Koen Van Den Abeele, who have contributed much to our theoretical understanding of the phenomena described here. We also thank K. E.-A. Van Den Abeele, the two reviewers, and the Assistant Editor who did much to clarify the text.

References

Guyer, R. A., K. R. McCall, and G. N. Biotnott, Hysteresis, discrete memory and nonlinear wave propagation in rock, *Phys. Rev. Lett.*, *74*, 3491–3494, 1994.

Guyer, R. A., K. R. McCall, P. A. Johnson, P. N. J. Rasolofosaon, and B. Zinszner, Equation of state hysteresis and resonant bar measurements on rock, in *International Symposium on Rock Mechanics*, edited by J. J. K. Daemon and R. A. Schultz, pp. 177–181, A. A. Balkema, Rotterdam, Netherlands, 1995.

Hamilton, M. F., Fundamentals and applications of nonlinear acoustics, in *Nonlinear Wave Propagation in Mechanics—AMD-77*, Am. Soc. of Mech. Eng., New York, 1986.

Johnson, P. A., and P. N. J. Rasolofosaon, Nonlinear elasticity and stress-induced anisotropy in rock, *J. Geophys. Res.*, *101*, 3113–3124, 1996a.

Johnson, P. A., and P. N. J. Rasolofosaon, Manifestation of nonlinear elastic in rock: Convincing evidence over large frequency and strain intervals from laboratory studies, *Nonlinear Proc. Geophys.*, *3*, 77–88, 1996b.

Johnson, P. A., B. Zinszner, and P. N. J. Rasolofosaon, Resonance and nonlinear elastic phenomena in rock, *J. Geophys. Res.*, *101*, 11,553–11,564, 1996.

Kadish, A., P. A. Johnson, and B. Zinszner, Evaluating dynamic hysteresis in Earth materials, *J. Geophys. Res.*, *101*, 25,139–25,147, 1996.

Lucet, N., P. N. J. Rasolofosaon, and B. Zinszner, Sonic properties of rock under confining pressure using the resonant bar technique, *J. Acoust. Soc. Am.*, *89*, 980–990, 1991.

McCall, K. R., and R. A. Guyer, Equation of state and wave propagation in hysteretic nonlinear elastic materials, *J. Geophys. Res.*, *99*, 23,887–23,897, 1994.

Meegan, G. D., P. A. Johnson, R. G. Guyer, and K. R. McCall, Observations of nonlinear elastic wave behavior in sandstone, *J. Acoust. Soc. Am.*, *94*, 3387–3391, 1993.

Murphy, W. F., III, Effects of microstructure and pore fluids on the acoustic properties of granular sedimentary materials, Ph.D. dissertation, Stanford Univ., Stanford, Calif., 1982.

Shamina, O. C., A. M. Palenov, Z. Stopinskiy, V. S. Tkachenko, and N. A. Yakushina, Influence of ultrasonic vibrations on physicomechanical properties of rocks, *Izv. Acad. Sci. USSR Phys. Solid Earth*, Engl. Transl., *26*, 694–699, 1990.

Ten Cate, J. A., and T. J. Shankland, Slow dynamics in the nonlinear elastic response of Berea sandstone, *Geophys. Res. Lett.*, *23*, 3019–3022, 1996.

Ten Cate, J., K. Van Den Abeele, T. J. Shankland, and P. A. Johnson, Laboratory study of linear and nonlinear elastic pulse propagation in sandstone, *J. Acoust. Soc. Am.*, *100*, 1383–1391, 1996.

Van Den Abeele, K. E.-A., Elastic pulsed wave propagation in media with second or higher order nonlinearity, 1, Theoretical framework, *J. Acoust. Soc. Am.*, *99*, 3334–3345, 1996.

Van Den Abeele, K. E.-A., P. A. Johnson, R. A. Guyer, and K. R. McCall, On the analytical solution of hysteretic nonlinear response in elastic wave propagation, *J. Acoust. Soc. Am.*, *101*, 1–14, 1997.

Winkler, K., A. Nur, and M. Gladwin, Friction and seismic attenuation in rocks, *Nature*, *277*, 528–531, 1979.

P. A. Johnson, Earth and Environmental Science Division, MS D443, Los Alamos National Laboratory, Los Alamos, NM 87545. (e-mail: johnson@seismo5.lanl.gov)

P. N. J. Rasolofosaon and B. Zinszner, Institut Français du Pétrole, B.P. 311-92506, Rueil Malmaison Cedex, France. (e-mail: patrick.rasolofosaon@ifp.fr; bernard.zinszner@ifp.fr)

(Received January 18, 1996; revised October 10, 1996; accepted October 15, 1996.)